PROCEEDINGS B

royalsocietypublishing.org/rspb

Research

Cite this article: Miller T, Rogers S, Wu J, Cicirello A, Taylor GK, Mortimer B. 2026 Spider leg biomechanics as an information filter for vibration sensing. *Proc. R. Soc. B* **293**: 20260915.
https://doi.org/10.1098/rspb.2026.0915

Received: 4 July 2025
Accepted: 13 May 2026

Subject Category:
Morphology and biomechanics

Subject Area:
biomechanics

Keywords:
vibration, localization, mechanosensor, spider

Author for correspondence:
Thomas Miller
e-mail: thomas.miller@biology.ox.ac.uk

Electronic supplementary material is available online at https://doi.org/10.6084/m9.figshare.c.8510006.

THE ROYAL SOCIETY
PUBLISHING

Spider leg biomechanics as an information filter for vibration sensing

Thomas Miller[1], Stephen Rogers[1], Jun Wu[1,2], Alice Cicirello[3],
Graham Keith Taylor[1] and Beth Mortimer[1]

[1]Department of Biology, University of Oxford, Oxford OX1 3EL, UK
[2]School of Metallurgy and Materials, College of Engineering and Physical Sciences, University of Birmingham, Birmingham, B15 2SE, UK
[3]Department of Engineering, University of Cambridge, Cambridge CB2 1PZ, UK

TM, 0000-0002-9647-570X; JW, 0000-0003-4817-6454; GKT, 0000-0001-8289-755X;
BM, 0000-0002-7230-3647

Substrate-borne vibration sensing is an important sensory modality in arthropods, which use externally generated vibration sources to gather information about their environment. Vibrations are subject to mechanical filtering by the legs and body, which implicates a role for morphology in modulating information flow due to the distributed and embedded nature of arthropod mechanosensors. A general problem with sensing is the separation of signal from noise. While internally generated vibrations can be useful for proprioception, they potentially obscure the small displacements generated by substrate vibrations for exteroception. Here, we use a laser vibrometry dataset quantifying the dynamic response of the tarantula *Grammostola pulchra* to vibrational input at 50 points across its legs and body to examine relative motion in a single axis, enabling us to infer leg biomechanics and test whether these behave rigidly as vibrations are transmitted through the body. We show that the non-rigid legs may dampen large-amplitude motion from cephalothorax/abdomen resonance—increasing signal-to-noise ratio for exteroception at their distal ends. These properties may also act to increase the robustness of vibration sensing to variation in morphological traits affecting the spider's dynamics. As spider body plans are conserved, we argue the results are generalizable across the mechanosensitive Araneae.

1. Introduction

Substrate-borne vibrations are ubiquitous in the environment and are an important information source for animals—particularly arthropods, for which substrate-borne vibration sensing is an ancient and basal modality [1,2]. Vibrations provide biologically relevant information in the form of signals and cues—arthropods use these for conspecific communication (such as courtship) [3–7], detecting prey [8–11], avoiding predators [12] and assessing environmental variables [9,13].

Arthropods detect substrate-borne vibrations using embedded mechanosensors. In spiders, these mechanosensors include the slit sense organs, while insects have campaniform sensilla and chordotonal organs such as the subgenual organ [14]. When the arthropod's body vibrates, either due to internal or external perturbation, it leads to motion of some leg or body segments relative to each other. In turn, this generates cuticle deformation, producing strains which are measured by mechanosensors embedded within the exoskeleton [15]. These mechanosensors can be found across the body but are most apparent on the legs and wings [16–18]. Their distribution varies depending on interspecific differences in morphology, but some patterns in mechanosensor location are broadly conserved across taxa—e.g. in insect wings [17] and spider bodies [19–24]. Generally, levels of deformation have been shown to be highest in the areas of cuticle around the joints between moving segments—which is where arthropod mechanosensors are typically located.

Due to being embedded in the exoskeleton, arthropod mechanosensors detect vibration sources generated both externally (exteroception) and internally (interoception). For exteroception (i.e. directly measuring substrate motion), sensors located at the distal ends of the legs—at the animal-substrate interface—would theoretically minimize the distance between the source of interest (the substrate) and the sensor, so we would expect these to have the least ambiguous responses. In spiders, sensor placement and function have been extensively studied in the wandering spider *Cupiennius salei*, where the metatarsal lyriform organ (HS10) is thought to be particularly important for exteroception and is stimulated by relative motion of the tarsus and metatarsus in both a lateral and dorsoventral direction [25,26]. Spider lyriform organs in different locations (such as HS8 on the tibia), as well as hair plates spanning joints, have been implicated for proprioception [27–30]. While the electrophysiology of individual lyriform organs and behavioural response to vibrational stimulus are best understood in *Cupiennius*, due to the conserved body plan of most spiders (particularly at larger sizes), the general biomechanics are broadly comparable between even distantly related taxa, even if small details may vary between species. For example, previous work has used measurements from multiple species of tethered tarantulas (where strains in the exoskeleton can be easier to measure) to interpret the results of an experiment with freely walking *Cupiennius*, implying similar body dynamics and conserved function of the HS8 lyriform organ [15].

As well as being influenced directly by vibration sources, whether externally or internally generated, the cuticle deformation detected by mechanosensors is also affected indirectly by vibration sources due to resonances in the spider's whole body. The natural frequencies are the frequencies at which an object will tend to oscillate in the absence of ongoing external forces after a perturbation, and the corresponding mode shapes are the deformed shapes produced by the relative motion of different elements in a system. Resonance occurs when the frequency of an external periodic force matches the natural frequency, causing a substantial increase in vibration amplitude within the object. We would expect resonance-induced cuticle deformation to favour a narrow subset of signals detected by embedded sensors during exteroception since resonance amplifies motion at a particular frequency, like the sound of a bell ringing following an impact. This passive response is governed by the biomechanics of the body, including mass (particularly in the abdomen), the stiffness and damping of joints between segments [31] and overall geometry, as these affect a vibrating mechanical system's natural frequencies and mode shapes [32]. Arthropods, of course, are not passive mechanical machines, but can actively change some biomechanical parameters, and some are also affected by biological processes that might be expected to influence vibration sensing (e.g. growth, feeding, reproduction in the longer term; posture, muscle tension and even blood pressure in the short term) [32,33]. While the sensitivity and threshold curves of individual mechanosensors have been the subject of intense research, surprisingly little is known about the dynamics of the whole body under vibrational input—which is crucial for understanding how cuticle deformation stimulates the mechanosensors in a real-world context.

A more detailed investigation of arthropod body dynamics in a natural posture is crucial for understanding the underlying mechanisms of vibration sensing, with implications for arthropod sensory biology and biomechanics. The dynamics of different parts of the legs and body can be inferred from their relative motion (as a proxy for cuticle deformation) to determine the rigidity of the body/leg morphology and the potential roles of resonance. Measuring cuticle deformation directly, as mechanosensors do, is challenging in experimental contexts [34]. Relative motion of leg/body segments over time can be quantified using two variables—amplitude difference between the segments and phase delay between the segments. Amplitude differences between segments are modulated by the rate of energy loss of the source wave as it passes through both environmental substrates and the arthropod body. Phase delays are modulated by wavespeed, which is in turn governed by the material properties of the body and the substrate. These variables can be assessed in the frequency domain after conducting a modal test of the arthropod body under vibrational input. Joint bending, defined as the relative motion of adjacent leg/body segments, is assumed to be the primary reason why there are amplitude and phase delays between leg/body segments. Alternatively, bending of the leg/body segments themselves can contribute to this, but cuticular stiffness is much higher away from the more flexible joints [35]. For the purposes of this study, we will discuss relative motion between legs/body segments without assuming intra-joint bending explicitly.

Within arthropods, spiders are excellent model organisms for studying vibration sensing [36] as they are highly sensitive to vibrations—for most species, this is their primary sensory modality. Wu *et al.* [33] used a mass–spring–damper model (calibrated to the mode shapes of the tarantula spider *Grammostola pulchra* in its natural posture, derived experimentally using laser vibrometry) to investigate parameters influencing vertical vibration transmission through the spider body. In this model, each leg was simplified into a single mass–spring–damper unit (i.e. not considering relative motion of segments within each leg), which was an assumption that allowed the modelling of the entire body as a simple mass–spring–damper system in the vertical axis. This raises the question of whether relative motion of segments within a leg plays a role in spider vibration sensing, or whether a rigid-legged model is sufficient for explaining spider vibrational responses?

The aim of this study was to quantify the vibrational response of a live spider in its natural posture under vibration input, to investigate the extent of relative motion between segments across the body in the vertical axis. Relative motion, in turn, allows us to infer how spider biomechanics, specifically rigidity, influences spider vibration sensing. Our null hypothesis is that relative motion between leg segments is limited, with the leg moving as a rigid single unit that can be well-approximated with a mass-spring-damper, as assumed by the modelling approach in Wu *et al*. [33]. If non-rigid, we would expect the extent of relative motion to differ between the tarsus/metatarsus joint (implicated in exteroception due to mechanosensor placement) and the upper leg segments/cephalothorax. The patterns of relative motion across and between legs/body will give insights into whether and how spiders, as an example (and arthropods more generally), can use their biomechanics to help shape sensory information, particularly increasing signal-to-noise ratio for exteroception.

2. Methods

(a) Experimental set-up

We used one specimen of *G. pulchra* Mello-Leitão, 1921, from our captive lab population. The spiders were kept in plastic terrariums with a coir substrate and fed with crickets twice weekly, in a temperature-controlled room set at 20°C with a 12 h day/night cycle. *Grammostola pulchra* is native to southern Brazil and is ground-dwelling, sensing vibrations for hunting and courtship across a range of substrates (including soil, rock, leaf litter and wood). They build a retreat by burrowing into the soil and have a calm temperament, which makes them convenient for use in these experiments. We measured the mass of the spider using an Ohaus Pioneer mass balance and photographed the spider on the day of the experiment. Photos from three angles were used to produce a three-dimensional skeleton of the spider's body, which was later used for animation of the mode shapes [33].

The vibration stage consisted of a circular aluminium plate (95 mm diameter, 4 mm thickness) attached directly to the shaker (Modal Shop K2004E01) using a threaded bolt (figure 1). We measured the motion of this plate using an accelerometer (PCB 352A21) attached to the bottom of the aluminium plate. The dimensions of the plate were chosen to avoid resonances at lower frequencies that would influence the response of the spider body, and this was verified by measuring the response of the plate without the spider present.

The aluminium plate was driven by a square wave voltage input in the vertical axis generated with a signal generator. The length of the square wave was approximately 0.0005 s. This pulse input was chosen for three reasons—the regular occurrence of impact signals in a biological context, the broadband excitation of frequencies in a biologically relevant range for the tarantula (up to 1000 Hz) and the fact that the duration of the input was short enough that it did not elicit a behavioural response in the spider.

The spider was guided towards the centre of the aluminium plate using forceps and left to acclimatize. The spider was not tethered or restrained in any way. If the spider moved, it was encouraged back to the centre using the forceps. After the spider had assumed a relaxed posture for around 10 min, the test was performed. During the dynamic test, the spider's posture was approximately bilaterally symmetrical, but from front to back legs, there were differences in posture—in particular, the front legs were more retracted during the test. If the spider moved, the experiment was restarted, until a full set of measurements could be taken, since the spider needed to remain still for the entirety of data collection.

A laser Doppler vibrometer (Polytec VibroOne) was used to measure the velocity of the spider's body in the vertical axis in response to vibrational input, with the laser set perpendicular to the aluminium plate. Recordings were taken in the time domain with a total length of 1.28 s. Our sampling frequency was 25.6 kHz. We manually focused the laser on 50 pre-determined vertical points on the spider's body, which are illustrated in figure 1. These points correspond approximately with areas experiencing high levels of cuticular strain at the joints between adjacent segments, where sensors are typically located. Measurements were not taken from the trochanter and coxa as these were obscured when the spider was in its natural posture. The laser was manually focused directly onto the cuticle of the spider without any reflective material attached to the body. The set-up allowed the angle of the laser beam to remain fixed at 90 degrees to the aluminium plate (the laser vibrometer mount moved in the horizontal plane), and hence the motion measured by the laser vibrometer is the vertical motion of the measurement point relative to the vibration input. Since the measurement point was not fixed relative to the spider body, we consider it a floating reference frame. This technique adequately captures the dynamics of the spider body in the vertical axis, but there is the potential for measurement error caused by motion of body segments in the horizontal axis. We assume that these displacements are minor relative to motion in the vertical axis due to the pulse input being confined to the vertical axis.

We generated the pulse input three times after focusing the laser on each measurement point, taking a new recording each time. After three repeats were taken for each measurement point, we moved the laser vibrometer to the next point and repeated the process until data was collected from all 50 points.

The coherence of the measurement can be used to assess the signal-to-noise ratio at different frequencies. In an ideal constant parameter linear system with a single input and single output, the coherence would be close to 1, therefore enabling us to accurately capture the complete system dynamics. The coherence is equal to zero when the input and output are completely unrelated. We retained data on signal quality, and noisy recordings with low coherence were discarded—only high-quality recordings were used in our analysis. It was verified that the coherence of the retained measurements was mostly above 0.9 in the frequency range of interest, although a few leg segments and the abdomen showed slightly lower coherence—these segments are, however, retained in the graphs for comparison (see electronic supplementary material, figures S1–S3 for coherence graphs of each repeat).

(b) Data analysis

We used the accelerometer measurement of the aluminium plate as our input data and the vibrometer measurement of the spider's body as our output response. A Tukey window with a cosine taper of 10% was applied to the input and output data in the time domain, to smooth the start and end of the recording to zero while preserving the amplitude of the signal for the duration of the input pulse. The data were then converted to the frequency domain using a discrete Fourier transform (DFT). A frequency response function (FRF), expressing the magnitude and phase of the output DFT relative to the input DFT, was calculated for each point on the spider using the modalfrf function in Matlab. We used the sensor argument 'dis' in modalfrf so that the function did not automatically transform the input/output. We then took the mean of the FRFs of each of the three

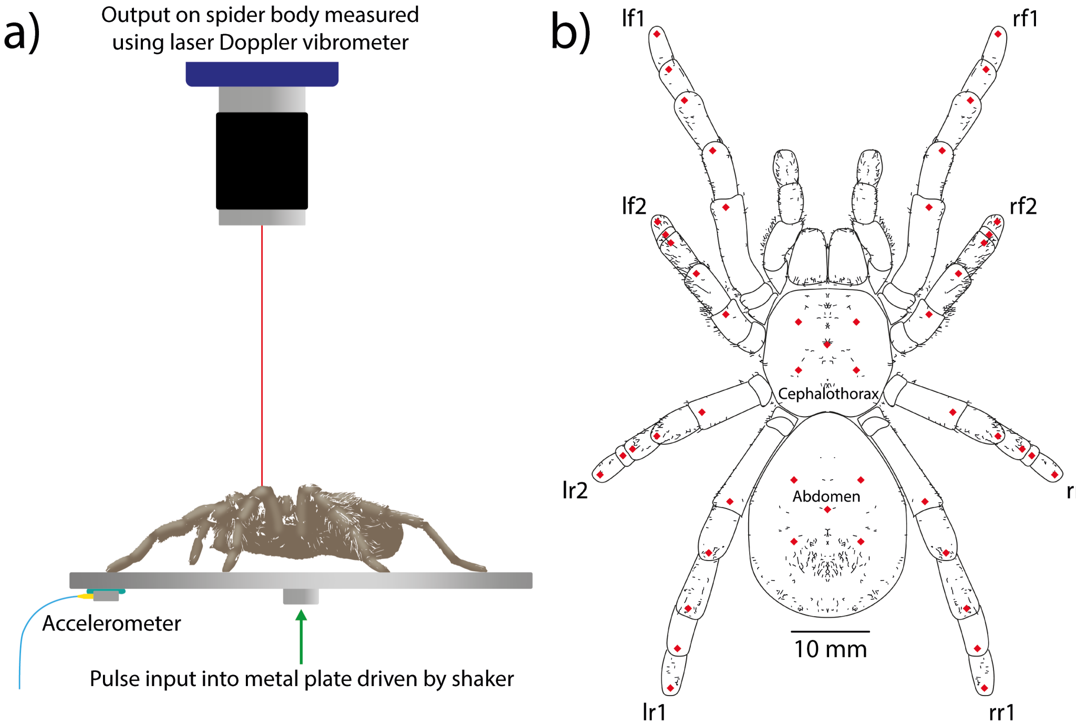

Figure 1. Experiment: (a) set-up; (b) vertical measurement points on the spider. This figure is used for illustration of all the measurement points, given by the red dots in (b). Note that the posture shown here is not the same as the test. During experiments, spiders were not anaesthetized or tethered, but a vertical tube was used to enclose the spider from above and prevent escape from the arena, where the tube did not touch the aluminium plate. Reproduced from Wu *et al.* [33] under CC BY 4.0 License for open access publications in the Journal of the Royal Society Interface.

repeats for each point to calculate a single average FRF. For 3 out of the 50 measurement points, the input accelerometer measurement in one of the repeats was unusable due to equipment error, resulting in a very low coherence, so the average FRF was calculated by taking the mean of the other two repeats.

The disadvantage of a pulse input in terms of FRF analysis is that all frequencies are excited simultaneously, so the measured response of the spider body at a particular frequency is, in fact, the response to that frequency and any superimposed harmonics associated with lower frequencies. However, harmonic content arises from nonlinearity, and given the low amplitude of the pulse, it is reasonable to assume that the relationship between input and output is linear over the frequency range considered, and any nonlinear effects will be negligible.

During the experiment, we judged the spider's posture to be approximately bilaterally symmetrical, so we assumed that the average FRFs obtained for measurement points on symmetrical leg segment pairs would retain bilaterally symmetrical properties. As a result of this assumption, the FRFs obtained for symmetrical leg segment pairs could be exploited to highlight inherent differences in response that would enable the spider to locate the vibration source.

To quantify differences in the frequency response between measurement points, we calculated the mean squared error (MSE) of the average FRFs obtained at each bilateral pair of legs (e.g. lr1/rr1), between the tarsus of each leg and all other segments, between the cephalothorax and all other segments in each leg and between adjacent segments in each leg (electronic supplementary material, table S1). With this global metric, the lower the MSE, the greater the degree of similarity between the FRFs. We reproduce the full MSE values in the electronic supplementary material (electronic supplementary material, table S1).

Wu *et al.* [33] used a version of this dataset consisting of only one repeat (without taking an average FRF) to calibrate a simple 11 degrees of freedom mass–spring–damper model of the spider body, in order to probe variables influencing vibration sensing through parametric tests. The model was constructed in Matlab using Simulink. Full details of this method are given in that study, but in brief—a PolyMAX algorithm was first used to identify the natural frequencies of the entire spider system from our 50 measured points across the body. In total, five natural frequencies were identified—at 31.75, 37.65, 74.15, 108.43 and 137.41 Hz. Then, the natural frequencies and damping ratios of the model were calibrated to the real system, while also attempting to ensure that the mode shapes and FRFs showed a satisfactory match. A limitation of our experimental strategy is that we were not able to apply a sinusoidal input closer or exactly at these calculated natural frequencies to the real spider to validate them, because persistent stimuli invoked a behavioural response.

3. Results

The frequency of the vibration input alters the resulting spider dynamics, which is quantified using an FRF (figure 2). When comparing equivalent leg segments, the results show that the characteristics of the FRFs at different frequency ranges are similar for all legs (figure 2). Below 20 Hz, the FRFs for all segments are dominated by noise, while above 200 Hz, the FRFs do not show obvious resonances and have low amplitude. Therefore, we only consider the 20–200 Hz frequency range, which mostly overlaps with the range where the sensitivity of the HS10 lyriform organ in *Cupiennius* is highest (>40 Hz) [37].

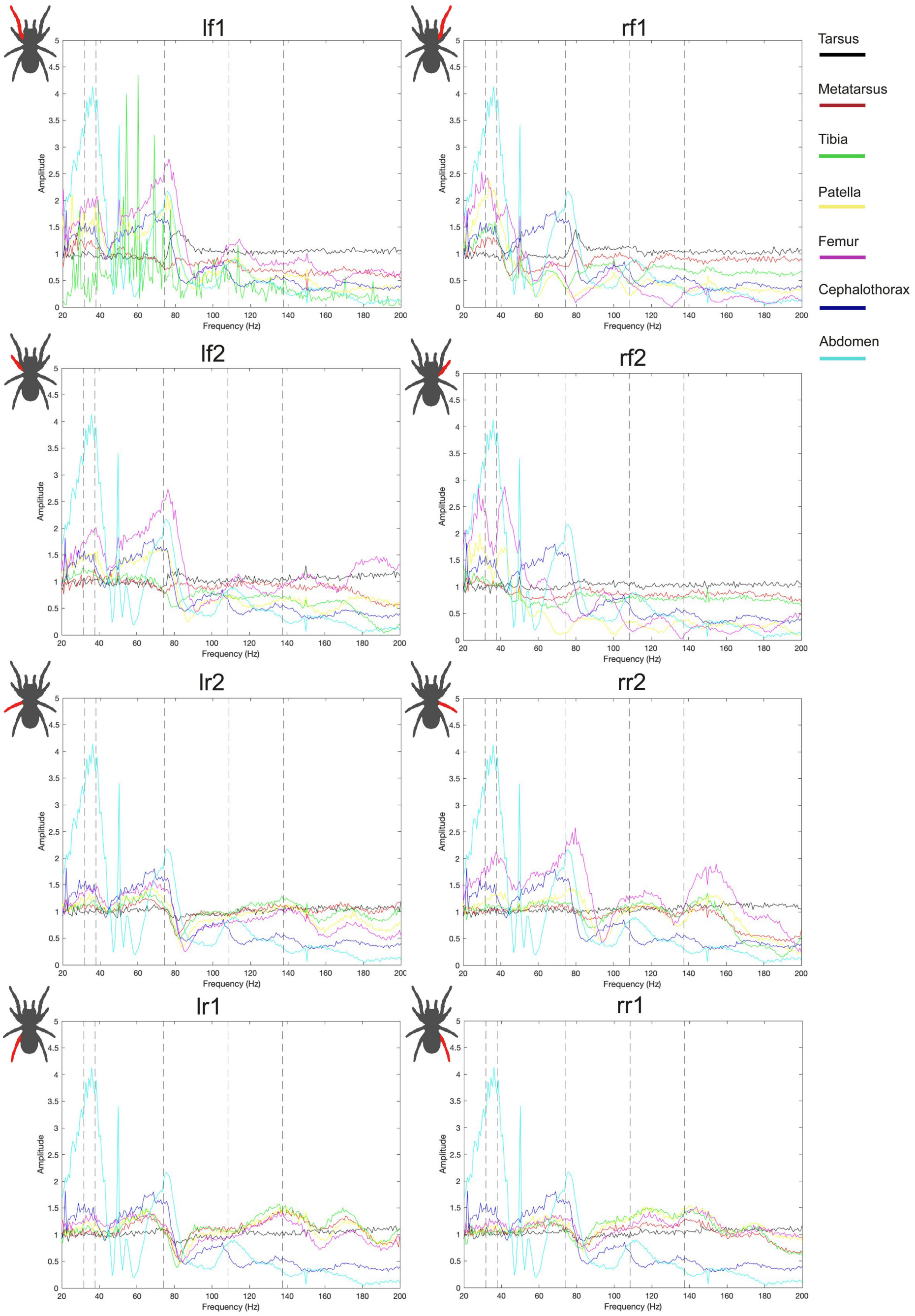

Figure 2. Magnitude of average FRFs for legs rr1, rr2, rf2, rf1, lr1, lr2, lf2 and lf1 calculated from the modal test in the range 20–200 Hz. Cephalothorax and abdomen plotted over each graph. Vertical dashed lines indicate the five modes of the spider body. A value of 1 (in arbitrary units) means that the output amplitude (leg motion) matches the input amplitude (vibration plate motion).

Figure 2 shows that the FRF magnitude (the y-axis deviation from 1, where 1 is a perfect match between vibration plate and measured spider motion) varies according to the leg or body segment that is measured. For the distal segments (e.g. tarsus and metatarsus), the magnitude of FRFs remains close to 1 across 20–200 Hz, indicating the amplitude of motion is similar to the vibration plate. However, for the cephalothorax, abdomen and proximal leg segments, between 20 and 80 Hz, the magnitude of the FRFs is greater than the distal leg segments with an amplitude value of greater than 1—which refers to a higher amplitude of motion relative to the plate input at these frequencies. In contrast, above 80 Hz, there is a sudden decline in the magnitude of the response in the proximal leg segments, cephalothorax and abdomen, with the response falling below the magnitude of the distal leg segments with values less than 1—indicating lower amplitude of motion relative to the plate input and the opposite of the pattern observed in the 20–80 Hz range. This drop-off after the amplitude peak at approximately 80 Hz is associated with the third mode of the spider body [33]. Due to some asymmetry in the rearmost legs, the tibia, patella and femur of lr1 and lr2 do not follow this pattern.

In addition, the phase also differs according to the leg or body segment that is measured and the frequency range considered (figure 3). Distal segments have phase values close to π radians at all frequencies, indicating they are in phase with the vibration plate (i.e. their up-down motions are synchronized). The phase of the abdomen and cephalothorax suddenly decreases by 2–4 radians above 80 Hz, before increasing slightly at 100 Hz—above which it decreases again. This indicates that at these higher frequencies, the motion of these segments is out of phase with the distal leg segments and the vibration plate (figure 3). The

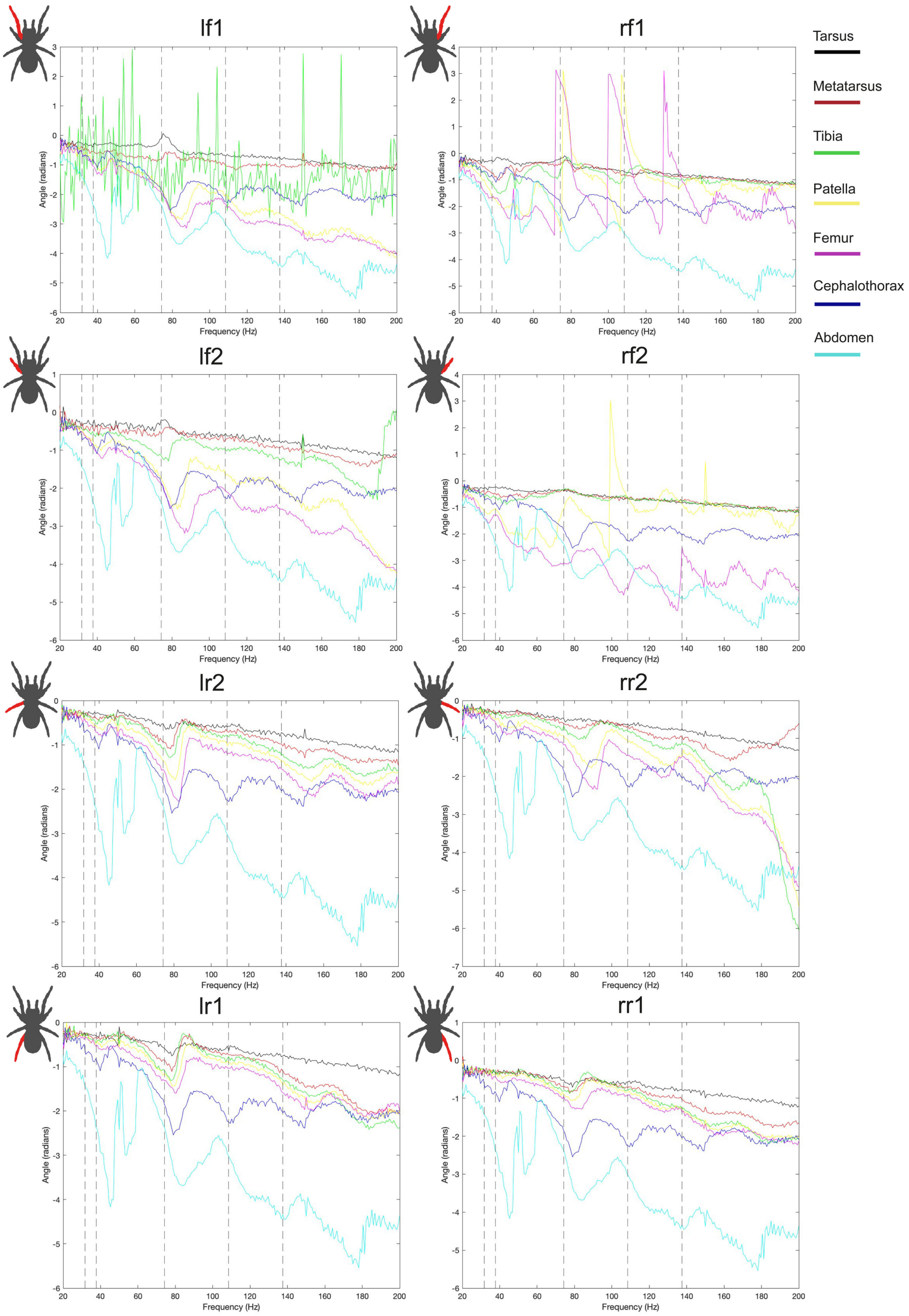

Figure 3. Phase of average FRFs for legs rr1, rr2, rf2, rf1, lr1, lr2, lf2 and lf1 calculated from the modal test in the range 20–200 Hz. Cephalothorax and abdomen plotted over each graph. Vertical dashed lines indicate the five modes of the spider body. A value of approximately 3.14 (π) means that the output phase (leg motion) matches the input phase (vibration plate motion).

extent to which the abdomen and cephalothorax are out of phase with the rest of the body in this higher frequency range varies depending on the leg segment measured and the exact frequency considered, but typically lags by 1–4 radians. This will lead to increased relative motion above this frequency range, particularly in the proximal leg segments near the attachment to the cephalothorax. The phase delays between each body segment are approximately correlated with distance from the coupling points with the substrate, i.e. increased delays moving from distal to proximal segments—which is also correlated with increasing mass of these segments towards the abdomen.

By calculating the mean squared error (MSE) (electronic supplementary material, table S1), we quantified the expected variation in FRFs between symmetrical leg segment pairs (based on the *a priori* assumption that if the spider's posture and each measurement point was perfectly symmetrical, then the MSE would be 0), enabling us to highlight inherent differences in response due to biomechanical parameters that are outside this expected level of variation.

Generally, there is more of a difference between the cephalothorax/abdomen and distal leg segments than there is in symmetrical left/right leg segment pairs in the FRFs, indicating that we can interpret these comparisons with a high level of confidence. For the rear two leg pairs (lr2/rr2 and lr1/rr1), the MSE between equivalent left/right leg segments is consistently an order of magnitude lower than between the cephalothorax and all the leg segments apart from an asymmetry in the FRFs of the femur. For the front two pairs of legs (lf1/rf1 and lf2/rf2), there is a much greater degree of bilateral asymmetry across most leg segments, but the MSE between the cephalothorax and the distal leg segments (tarsus/metatarsus) remains higher than the left/right comparison, indicating that we can still usefully interpret differences in the FRFs. A possible reason for these asymmetries could be poor coherence (<0.6) at some measurement points (electronic supplementary material, figures S1–S3), indicating more noise and/or nonlinearity between the input and the output, e.g. in the tibia of rr1, and possibly the patella and femur in lr1.

Overall, the results support that the legs are not acting rigidly, since both FRF magnitude and phase differ between leg segments. This indicates relative motion between the leg segments, with a smooth transition in dynamics from the distal end behaving more like the plate and the proximal end behaving more like the body resonance. There is no stark transition across any particular segment indicated in our data from *Grammostola*. We can therefore reject our null hypothesis, as we do not find data to support that the legs behave in a way that can be well-approximated with a mass–spring–damper unit, where we would expect to see no differences in phase or FRF magnitude due to rigid acting legs on a suspended mass.

4. Discussion

Many arthropods rely heavily on exteroception of substrate-borne vibrations for prey capture, predator avoidance and courtship. The embedded nature of arthropod mechanosensors means that the links between material properties and dynamics of the body in response to vibrational input are an intrinsic part of the mechanisms underlying vibration-based exteroception. Here, we explore the relevance of this intrinsic property of biomechanical systems in the context of substrate-borne vibration sensing, by interpreting the resonances measured in the tarantula *G. pulchra* and comparing it with published data on other spiders and arthropods.

(a) The role of resonance in vibration sensing

Our results show that the frequency range that is most likely to be influenced by body resonance (and the associated modal shapes for the expected first five modes; see dashed lines in figure 2) for *G. pulchra* is between 20 and 200 Hz. This range overlaps with biologically relevant vibration sources from prey and courtship. Vibrations generated by walking insects are typically broadband in frequency content with peaks up to 1000 Hz (dependent on the transmission properties of the surface over which the prey is walking), while courtship vibrations in *Cupiennius* are lower frequency, with prominent peaks in the <150 Hz range [38]. While spider mechanosensors are theoretically capable of detecting frequencies below 20 Hz [26,29], frequencies in this range are mainly generated by environmental noise such as wind, so may have less biological importance for exteroception. Indeed, in *Cupiennius* spiders, these low frequencies are subjected to high-pass mechanical filtering by the cuticular pad [39]. These results are comparable to those reported previously, which indicate limited mechanosensor sensitivity for frequencies below approximately 30 Hz in *Cupiennius* [26], and body modes present at relatively low frequencies (18 and 63 Hz) [38,40].

The transfer function of vibrations through the body of the large hunting spider *Cupiennius getazi* (body length approximately 2.6 cm) was broadly similar to those exhibited by *G. pulchra* (in this study, though, vibrations were delivered via the medium of a bromeliad leaf, the usual habitat of *Cupiennius*) [41]. *Cupiennius* showed resonant amplification across a broader range of frequencies, from <1 up to 200 Hz, with a peak amplification at approximately 80 Hz, compared with the 20–80 Hz range and 35 Hz peak amplification shown by *Grammostola*. In *Cupiennius,* frequencies above 200 Hz were attenuated, similar to higher frequency responses of *Grammostola*. The two spider species also demonstrated a similar relative motion across different leg segments, with the response of the tarsi (where the spider body couples to the substrate) resembling the response of the substrate, and segments more proximal deviating significantly from this, and the opisthosoma showing the most resonance—although the differences appeared less extreme in *Cupiennius* compared with *Grammostola*.

There are two possible ways to interpret the biological relevance of these results. The first is that resonance of the body (here cephalothorax/abdomen, where the mass of the spider body is concentrated) could be used for vibration sensing functions, e.g. source localization. In support of this, our results show that different leg segments resonate at approximately the same frequencies. Electrophysiology recordings have also shown that most slit sense organs in *Cupiennius* are broadly tuned, with HS10 being highly sensitive above approximately 10 Hz to at least 1000 Hz [26,28,42,43]. Theoretically, the direction and magnitude of body motion relative to the legs during resonance could be used by the spider to provide directional information for source localization, in the absence of direction-informative frequency cues due to the broad mechanosensor tuning.

However, we suggest that for spiders, body resonance is unlikely to be useful for exteroceptive vibration sensing when substrate vibration frequencies overlap with an arthropod’s natural frequencies. Within spiders, amplifying biologically relevant signals has been suggested as a potential role for body resonance [32,33,36]. However, we argue that the evidence here points towards the spider prioritizing exteroceptive functions at the leg tips. Large-amplitude vibrations of the body at its natural frequencies may mask the small deflections at the distal joints caused by externally generated vibrations passing from substrate to body. This is a physical constraint on information propagation in this system [44]. We suggest that the patterns of relative motion observed in our results are used as a frequency-dependent damping effect, which is most pronounced at the low frequencies at which the abdomen and cephalothorax resonate. This decreases the influence of this body resonance on motion at the distal joints (here tarsus/metatarsus joint) and hence reduces masking and distortion in the context of exteroception. Rather than behaving rigidly, the legs move flexibly under vibrational input, separating motion of the abdomen/cephalothorax from the distal leg tips. The tarsus/metatarsus joint is furthest from this centre of mass resonance, while being closest to the substrate and thus transmits externally generated vibrations to the HS10 metatarsal mechanosensor with high efficacy. We interpret this as a way for the spider to ‘listen in’ to the subtle frequency–amplitude–time content of the substrate vibration without being masked by the overriding 'ringing bell' of body resonance. This filtering property can presumably be controlled through posture, as this will alter the extent of relative motion between leg segments.

Our findings contrast with what has been proposed for other arthropod species. The non-hearing cave cricket (*Troglophilus neglectus*) makes extensive use of vibratory communication. In contrast to *Grammostola* and the examples above, the most pronounced resonant signal amplification was found in the tibia, the location of the vibration-sensitive subgenual organ. Minimal signal amplification occurred more distally in the metatarsus, and considerable attenuation was found more proximally in the femur [45]. Signal amplification was restricted to a relatively narrow band of frequencies, which varied systematically with the degree of flexion of the femoral–tibial joint, with peak amplification occurring at 900 Hz and 30° leg angle, down to 192 Hz at 150°. Sansom *et al.* [46] compared vibrational gain at the proximal tibia to the tarsus (the thorax or abdomen was not measured) in termite and ant species, finding that gain in termites occurred at lower frequencies (< 2.25 kHz) compared with ants (1.9–3.1 kHz), a difference they ascribe to the different leg proportions in these two groups of insects.

The bodies of fiddler crabs (*Uca pugilator*) likewise act as a filter and selective amplifier to vibration [47]. Low frequencies (25–250 Hz) were amplified, while frequencies above this range were mostly attenuated except for a small amplification at the highest frequencies examined (800–1000 Hz). As with *Grammostola*, these effects became more pronounced the closer to the centre of the body the measurements were taken, being greatest when measured from the carapace and weakest at the dactyl (equivalent to the tarsus). Intriguingly, a small postural change which reliably occurred in response to male drumming-like stimuli resulted in a more sharply tuned response with a narrower zone of amplification, whereas resting postures, with the carapace contacting the substrate, resulted in a broadening and flattening of the transfer function across the entire body.

In the treehopper *Umbonia crassicornis* (Hemiptera: Membracidae), pronounced resonant amplification was found in the thorax and femur to frequencies between 500 and 700 Hz, but there was considerable and increasing attenuation to frequencies above 1000 Hz [48]. The response of the tarsus, however, mirrored that of the vibrating substrate. In this animal, there is both a translational and rotational vibrational mode, so that the degree of amplification depended on the direction of travel of the vibrational wave, potentially giving this small insect the means to determine the origin of a signal even though amplification is most pronounced at the midline of the body.

In fact, the only equivalent example we could find where resonances are not found in the location of the mechanosensors in a biologically relevant range is in the honey bee (*Apis mellifera*), where no substantial resonance or attenuation at all was found in the proximal tibia in a tested range between 100 and 2000 Hz, despite the known importance of vibrational communication in this species [49].

Resonance is counteracted by damping, which is any mechanism, such as internal friction, that acts to dissipate the energy in an oscillating system. In critically damped or overdamped systems, no oscillation is possible. It is likely that the slit sensilla themselves are highly damped, since, otherwise, brief periods of stimulation could cause ongoing oscillation and neural activation even after the stimulus has stopped. Underdamped systems, however, still oscillate but with an exponentially declining amplitude over time. This can still allow for some moderate resonant amplification but typically the resonance peak is flattened and widened, with a small amplification occurring across a wider range of frequencies rather than a large amplification to a specific frequency. The FRFs of whole arthropods to vibration, including *Grammostola,* suggest that arthropod bodies generally act like moderately underdamped systems, potentially allowing the benefit of some amplification across a range of useful frequencies, but not subject to large resonances that risk overwhelming sensitive mechanosensory detectors.

The damping effect of the upper leg segments also means that fluctuations in the size, mass and density of the abdomen (e.g. from feeding/reproduction) have less of an impact on the relative motion of the distal leg joints. Therefore, this is an inherent property of the system that makes exteroception more robust to variation—a form of morphological computation, where information processing may be outsourced to morphology instead of the central nervous system (CNS). Mechanical filtering, for example, by the cuticular pad in spiders, can be considered morphological computation if it reduces the level of potential energy expenditure in the CNS [44,50]. A stronger argument for morphological computation could be made by showing that these parameters are actively controlled by spiders, e.g. through posture, which is a promising area for further studies given the frequency response of *U. pugilator* when changing posture [47].

(b) Outlook

Our findings can be generally applied to the concept of mechanosensor networks in sensory ecology. The implication is that a network of many simple mechanosensors is sufficient for vibration sensing, with the distribution of sensors and patterns of relative motion (modulated by morphological traits such as joint stiffness/damping) being important factors influencing vibration sensing. By positioning mechanosensors for exteroception close to the distal tips of the legs, arthropods are able to minimize internally generated noise due to damping body resonance through the upper leg segments, and thus mitigate against this biomechanical constraint. Evolutionarily, this opens questions into how arthropod bodies have evolved as multi-functional structures for vibration transmission and sensing, while preserving functions such as locomotion, feeding and reproduction.

Ethics. This work did not require ethical approval from a human subject or animal welfare committee.

Data accessibility. Our Grammostola pulchra modal test dataset (consisting of accelerometer input measurement, laser vibrometry output measurement and frequency response function), as well as the code used to generate the FRFs and plot the data, are available on Zenodo [51]. Supplementary material is available online [52].

Declaration of AI use. We have not used AI-assisted technologies in creating this article.

Authors' contributions. T.M.: conceptualization, data curation, formal analysis, investigation, methodology, software, validation, visualization, writing—original draft, writing—review and editing; S.R.: conceptualization, writing—original draft, writing—review and editing; J.W.:

conceptualization, data curation, investigation, methodology, software, writing—review and editing; A.C.: conceptualization, funding acquisition, methodology, project administration, supervision, writing—review and editing; G.K.T.: conceptualization, funding acquisition, methodology, project administration, supervision, writing—review and editing; B.M.: conceptualization, funding acquisition, methodology, project administration, supervision, writing—review and editing.

All authors gave final approval for publication and agreed to be held accountable for the work performed therein.

Conflict of interest declaration. We declare we have no competing interests.

Funding. This work was supported by the Royal Society University Research Fellowship (grant no. URF\R1\191033).

Acknowledgements. We thank the animal technicians for their valued contributions to spider husbandry. For help with experimental set-ups, we thank John Hogg.

References

1. Cocroft RB, Rodríguez RL. 2005 The behavioral ecology of insect vibrational communication. *Bioscience* **55**, 323–334. (doi:10.1641/0006-3568(2005)055[0323:TBEOIV]2.0.CO;2)
2. Hill PSM. 2019 What is biotremology? In *Biotremology: studying vibrational behavior* (ed. PSM Hill), pp. 15–25. Berlin, Germany: Springer. (doi:10.1007/978-3-030-22293-2_2)
3. Schuch W, Barth FG. 1985 Temporal patterns in the vibratory courtship signals of the wandering spider *Cupiennius salei* Keys. *Behav. Ecol. Sociobiol*. **16**, 263–271. (doi:10.1007/BF00310990)
4. Schuch W, Barth FG. 1990 Vibratory communication in a spider: female responses to synthetic male vibrations. J. Comp. Physiol. A Neuroethol. Sens. Neural Behav. Physiol. **166**, 817–826. (doi:10.1007/BF00187328)
5. Hunt RE, Morton TL. 2001 Regulation of chorusing in the vibrational communication system of the leafhopper *Graminella nigrifrons*. *Am. Zool*. **41**, 1222–1228. (doi:10.1093/icb/41.5.1222)
6. Elias DO, Mason AC, Maddison WP, Hoy RR. 2003 Seismic signals in a courting male jumping spider (Araneae: Salticidae). *J. Exp. Biol*. **206**, 4029–4039. (doi:10.1242/jeb.00634)
7. Elias DO, Hebets EA, Hoy RR, Mason AC. 2005 Seismic signals are crucial for male mating success in a visual specialist jumping spider (Araneae: Salticidae). *Anim. Behav*. **69**, 931–938. (doi:10.1016/j.anbehav.2004.06.024)
8. Klarner D, Barth FG. 1982 Vibratory signals and prey capture in orb-weaving spiders (*Zygiella x-notata*, *Nephila clavipes*; Araneidae). *J. Comp. Physiol*. **148**, 445–455. (doi:10.1007/BF00619783)
9. Masters WM. 1984 Vibrations in the orbwebs of *Nuctenea sclopetaria* (Araneidae). 2. Prey and wind signals and the spider's response threshold. *Behav. Ecol. Sociobiol*. **15**, 217–223. (doi:10.1007/BF00292978)
10. Pfannenstiel RS, Hunt RE, Yeargan KV. 1995 Orientation of a hemipteran predator to vibrations produced by feeding caterpillars. *J. Insect Behav*. **8**, 1–9. (doi:10.1007/BF01990965)
11. Landolfa MA, Barth FG. 1996 Vibrations in the orb web of the spider *Nephila clavipes*: cues for discrimination and orientation. J. Comp. Physiol. A Sens. Neural Behav. Physiol. **179**, 493–508. (doi:10.1007/BF00192316)
12. Cocroft RB. 1996 Insect vibrational defence signals. *Nature* **382**, 679–680. (doi:10.1038/382679a0)
13. Casas J, Bacher S, Tautz J, Meyhöfer R, Pierre D. 1998 Leaf vibrations and air movements in a leafminer–parasitoid system. *Biol. Control* **11**, 147–153. (doi:10.1006/bcon.1997.0593)
14. Strauß J, Stritih-Peljhan N. 2022 Vibration detection in arthropods: signal transfer, biomechanics and sensory adaptations. *Arthropod Struct. Dev*. **68**, 101167. (doi:10.1016/j.asd.2022.101167)
15. Blickhan R, Weihmann T, Barth FG. 2021 Measuring strain in the exoskeleton of spiders—virtues and caveats. J. Comp. Physiol. A Neuroethol. Sens. Neural. Behav. Physiol. **207**, 191–204. (doi:10.1007/s00359-020-01458-y)
16. Pringle JWS. 1938 Proprioception in insects II. The action of the campaniform sensilla on the legs. *J. Exp. Biol*. **15**, 114–131. (doi:10.1242/jeb.15.1.114)
17. Aiello BR, Stanchak KE, Weber AI, Deora T, Sponberg S, Brunton BW. 2021 Spatial distribution of campaniform sensilla mechanosensors on wings: form, function, and phylogeny. *Curr. Opin. Insect Sci*. **48**, 8–17. (doi:10.1016/j.cois.2021.06.002)
18. Dinges GF, Chockley AS, Bockemühl T, Ito K, Blanke A, Büschges A. 2021 Location and arrangement of campaniform sensilla in *Drosophila melanogaster*. *J. Comp. Neurol*. **529**, 905–925. (doi:10.1002/cne.24987)
19. Vogel H. 1923 Über die Spaltsinneorgane der Radnetzspinnen. *Jena. Z. Naturw*. **59**, 171–208.
20. Barth FG, Libera W. 1970 Illustrated catalogue of a spider's slit sense organs (*Cupiennius salei* Keys). *Z. Fur Morphol. Der Tiere* **68**, 343. (doi:10.1007/BF00376006)
21. Kropf C. 1998 Slit sense organs of Comaroma simonii Bertkau: a morphological atlas (Araneae, Anapidae). In *Proc. of the 17th European colloquium of arachnology Edinburgh 1997*, vol. **1998**, pp. 151–159, Buckinghamshire, UK: British Arachnological Society.
22. Ganske AS, Uhl G. 2018 The sensory equipment of a spider - a morphological survey of different types of sensillum in both sexes of *Argiope bruennichi* (Araneae, Araneidae). *Arthropod Struct. Dev*. **47**, 144–161. (doi:10.1016/j.asd.2018.01.001)
23. Seo JH *et al*. 2020 Lyriform vibration receptors in the web-building spider, *Nephila clavata* (Araneidae: Araneae: Arachnida). *Entomol. Res*. **50**, 586–593. (doi:10.1111/1748-5967.12470)
24. Miller TE, Taylor GK, Mortimer B. 2022 Slit sense organ distribution on the legs of two species of orb-weaving spider (Araneae: Araneidae). *Arthropod Struct. Dev*. **67**, 101140. (doi:10.1016/j.asd.2022.101140)
25. Barth FG. 1985 *Neurobiology of arachnids*. Berlin, Germany: Springer-Verlag.
26. Barth FG, Geethabali. 1982 Spider vibration receptors: threshold curves of individual slits in the metatarsal lyriform organ. *J. Comp. Physiol*. **148**, 175–185. (doi:10.1007/BF00619124)
27. Seyfarth EA, Barth FG. 1972 Compound slit sense organs on the spider leg: mechanoreceptors involved in kinesthetic orientation. *J. Comp. Physiol*. **78**, 176–191. (doi:10.1007/BF00693611)
28. Barth FG, Bohnenberger J. 1978 Lyriform slit sense organ: thresholds and stimulus amplitude ranges in a multi-unit mechanoreceptor. *J. Comp. Physiol*. **125**, 37–43. (doi:10.1007/bf00656829)
29. Bohnenberger J. 1981 Matched transfer characteristics of single units in a compound slit sense organ. *J. Comp. Physiol*. **142**, 391–402. (doi:10.1007/BF00605451)
30. Seyfarth EA, Gnatzy W, Hammer K. 1990 Coxal hair plates in spiders: physiology, fine structure, and specific central projections. *J. Comp. Physiol. A-Sens. Neural Behav. Physiol*. **166**, 633–642. (doi:10.1007/BF00240013)
31. Blickhan R. 1986 Stiffness of an arthropod leg joint. *J. Biomech*. **19**, 375–384. (doi:10.1016/0021-9290(86)90014-x)

32. Miller TE, Mortimer B. 2020 Control vs. constraint: understanding the mechanisms of vibration transmission during material-bound information transfer. *Front. Ecol. Evol*. **8**, 587846. (doi:10.3389/fevo.2020.587846)

33. Wu J, Miller TE, Cicirello A, Mortimer B. 2023 Spider dynamics under vertical vibration and its implications for biological vibration sensing. *J. R. Soc. Interface* **20**, 20230365. (doi:10.1098/rsif.2023.0365)

34. Barth FG, Ficker E, Federle HU. 1984 Model studies on the mechanical significance of grouping in compound spider slit sensilla (Chelicerata, Araneida). *Zoomorphology* **104**, 204–215. (doi:10.1007/BF00312032)

35. Vincent JFV, Wegst UGK. 2004 Design and mechanical properties of insect cuticle. *Arthropod Struct. Dev*. **33**, 187–199. (doi:10.1016/j.asd.2004.05.006)

36. Barth FG. 2021 A spider in motion: facets of sensory guidance. *J. Comp. Physiol. Neuroethol. Sens. Neural Behav. Physiol*. **207**, 239–255. (doi:10.1007/s00359-020-01449-z)

37. Erko M *et al*. 2015 Micro- and nano-structural details of a spider's filter for substrate vibrations: relevance for low-frequency signal transmission. *J. R. Soc. Interface* **12**, 20141111. (doi:10.1098/rsif.2014.1111)

38. Barth FG, Bleckmann H, Bohnenberger J, Seyfarth EA. 1988 Spiders of the genus *Cupiennius* Simon 1891 (Araneae, Ctenidae) 2. On the vibratory environment of a wandering spider. *Oecologia* **77**, 194–201. (doi:10.1007/BF00379186)

39. McConney ME, Schaber CF, Julian MD, Barth FG, Tsukruk VV. 2007 Viscoelastic nanoscale properties of cuticle contribute to the high-pass properties of spider vibration receptor (*Cupiennius salei* Keys). *J. R. Soc. Interface* **4**, 1135–1143. (doi:10.1098/rsif.2007.1000)

40. Mhatre N, Sivalinghem S, Mason AC. 2016 Posture controls mechanical tuning in the black widow spider mechanosensory system. *bioRxiv.* 484828.

41. Dierkes S, Barth FG. 1995 Mechanism of signal production in the vibratory communication of the wandering spider *Cupiennius getazi* (Arachnida, Araneae). J. Comp. Physiol. A Neuroethol. Sens. Neural. Behav. Physiol. **176**, 31–44. (doi:10.1007/BF00197750)

42. Speck J, Barth FG. 1982 Vibration sensitivity of pretarsal slit sensilla in the spider leg. *J. Comp. Physiol*. **148**, 187–194. (doi:10.1007/BF00619125)

43. Gingl E, Burger AM, Barth FG. 2006 Intracellular recording from a spider vibration receptor. *J. Comp. Physiol. Neuroethol. Sens. Neural Behav. Physiol*. **192**, 551–558. (doi:10.1007/s00359-005-0092-3)

44. Mortimer B. 2017 Biotremology: do physical constraints limit the propagation of vibrational information? *Anim. Behav*. **130**, 165–174. (doi:10.1016/j.anbehav.2017.06.015)

45. Stritih Peljhan N, Strauß J. 2018 The mechanical leg response to vibration stimuli in cave crickets and implications for vibrosensory organ functions. *J. Comp. Physiol. A* **204**, 687–702. (doi:10.1007/s00359-018-1271-3)

46. Sansom TM, Lai JCS, Halkon BJ, Evans TA, Oberst S. 2025 Termite vibration sensing: the chordotonal organs and their appendages. *Ecol. Evol*. **15**, e72287. (doi:10.1002/ece3.72287)

47. Aicher B, Markl H, Masters WM, Kirschenlohr HL. 1983 Vibration transmission through the walking legs of the fiddler crab, *Uca pugilator* (Brachyura, Ocypodidae) as measured by Laser Doppler Vibrometry. *J. Comp. Physiol.* **150**, 483–491. (doi:10.1007/bf00609574)

48. Cocroft RB, Tieu TD, Hoy RR, Miles RN. 2000 Directionality in the mechanical response to substrate vibration in a treehopper (Hemiptera: Membracidae: Umbonia crassicornis). *J. Comp. Physiol. A* **186**, 695–705. (doi:10.1007/s003590000123)

49. Rohrseitz K, Kilpinen O. 1997 Vibration transmission characteristics of the legs of freely standing honeybees. *Zoology* **100**, 80–84.

50. Barth FG. 2019 Mechanics to pre-process information for the fine tuning of mechanoreceptors. *J. Comp. Physiol. A Neuroethol. Sens. Neural. Behav. Physiol*. **205**, 661–686. (doi:10.1007/s00359-019-01355-z)

51. Miller T. 2026 Data for: Grammostola pulchra modal test. Zenodo (doi:10.5281/zenodo.19944684)

52. Miller T, Rogers S, Wu J, Cicirello A, Taylor GK, Mortimer B. 2026 Supplementary material from: Spider leg biomechanics as an information filter for vibration sensing. Figshare. (doi: 10.6084/m9.figshare.c.8510006)